Carbohydrate Polymers 112 (2014) 255–263

Contents lists available at ScienceDirect

Carbohydrate Polymers

journal homepage: www.elsevier.com/locate/carbpol

Nanostructured membranes based on native chitin nanofibers prepared by mild process

Ngesa Ezekiel Mushi[a], Nuria Butchosa[a], Michaela Salajkova[a], Qi Zhou[a,b], Lars A. Berglund[a,c,*]

[a] Department of Fiber and Polymer Technology, Royal Institute of Technology, SE-100 44 Stockholm, Sweden
[b] School of Biotechnology, Royal Institute of Technology, AlbaNova University Centre, SE-106 91 Stockholm, Sweden
[c] Wallenberg Wood Science Center, Royal Institute of Technology, SE-100 44 Stockholm, Sweden

ARTICLE INFO

Article history:
Received 20 February 2014
Received in revised form 7 May 2014
Accepted 12 May 2014
Available online 27 May 2014

Keywords:
Preparation
Chitin nanofiber
Structure
Nanopaper membranes
Mechanical properties
Bound protein

ABSTRACT

Procedures for chitin nanofiber or nanocrystal extraction from Crustaceans modify the chitin structure significantly, through surface deacetylation, surface oxidation and/or molar mass degradation. Here, very mild conditions were used to disintegrate chitin fibril bundles and isolate low protein content individualized chitin nanofibers, and prepare nanostructured high-strength chitin membranes. Most of the strongly '*bound*' protein was removed. The degree of acetylation, crystal structure as well as length and width of the native chitin microfibrils in the organism were successfully preserved. Atomic force microscopy and scanning transmission electron microscopy, showed chitin nanofibers with width between 3 and 4 nm. Chitin membranes were prepared by filtration of hydrocolloidal nanofiber suspensions. Mechanical and optical properties were measured. The highest data so far reported for nanostructured chitin membranes was obtained for ultimate tensile strength, strain to failure and work to fracture. Strong correlation was observed between low residual protein content and high tensile properties and the reasons for this are discussed.

1. Introduction

The exoskeleton of Crustaceans (crabs, lobsters, etc.) is an interesting nanostructured composite based on chitin microfibrils as the major load-bearing component. The native structure is hydrated and forms a hard, strong and tough composite mainly of chitin, calcium carbonate particles and proteins (Giraud-Guille, 1984; Neville, 1967; Raabe, Sachs, & Romano, 2005). During biosynthesis, protein-bound chitin microfibrils form a network template for mineral deposition (Neville, 1967). The α-chitin crystal has an axial modulus of around 60 GPa (Ogawa, Kimura, & Wada, 2011), and the diameter is from 2.5 to 6 nm (Blackwell & Weih, 1980). The fairly high modulus is due to the highly ordered extended chitin chain conformations in the microfibrils. The homopolymer chains have antiparallel arrangement of repeating β-(1→4) linked 2-acetamido-2-deoxy-D-glucans (Rudall, 1963). The chemical structure of the chitin polymer is related to cellulose with the hydroxy group replaced with an acetyl amino group on the *C*2 position of each repeating glucopyranose ring, and degree of acetylation on the *C*2 amine group is between 70 and 100% depending on the resources of chitin (Kjartansson, Zivanovic, Kristbergsson, & Weiss, 2006). Chitin nanofibers with structures different from the native chitin microfibril can be extracted from crustaceans. For instance, Ifuku et al. (2010) extracted chitin nanofibers with a diameter of 10–20 nm. The larger diameter compared with the pure chitin microfibril, indicates the presence of some residual proteins. The term "nanofiber" is in the present study used to distinguish nanofibers extracted by man from the smaller diameter chitin microfibril in the native organism. Chitin nanofibers are also longer, more flexible and less degraded than the highly crystalline chitin whiskers (Fan, Fukuzumi, Saito, & Isogai, 2012; Fan, Saito, & Isogai, 2010).

The annual waste of crustacean shells from food production is very large. The potential use of chitin from such waste material in applications such as packaging is therefore interesting. However, the mechanical property potential of man-made chitin nanofiber materials is unclear. Here, focus is on nanostructured chitin membranes prepared by filtration of hydrocolloidal suspensions. Many studies provide little detail in terms of stress–strain curves or discussion of deformation mechanisms. The chemical changes in

* Corresponding author at: Department of Fiber and Polymer Technology, Royal Institute of Technology, SE-100 44 Stockholm, Sweden. Tel.: +46 8 7908118; fax: +46 87908101.
E-mail address: blund@kth.se (L.A. Berglund).

http://dx.doi.org/10.1016/j.carbpol.2014.05.038

extracted chitin, such as deacetylation or oxidation of the surface molecules in chitin nanofibers (Fan et al., 2012; Fan et al., 2010), may influence mechanical properties of chitin materials, and is a consequence of the extraction protocols. The larger diameter of extracted nanofibers and the presence of proteins are influencing the intrinsic mechanical properties of the nanofibers, compared with native microfibrils. The term "native" is used to distinguish the present nanofibers from those based on regenerated or strongly modified chitin.

The structural properties of chitin nanofibers have been reported for chitin from crabs (Ifuku et al., 2009; Ifuku et al., 2010), prawns (Ifuku, Nogi, et al., 2011a), squid, tubeworms (Fan, Saito, & Isogai, 2008) and mushrooms (Ifuku, Nomura, Morimoto, & Saimoto, 2011b). Typical data for modulus E and tensile strength σ^* are $E = 3$ GPa and $\sigma^* = 44$ MPa (Ifuku & Saimoto, 2012) to $E = 5$ GPa and $\sigma^* = 140$ MPa (Fan et al., 2012). Nanostructured chitin membranes based on chitin-protein nanofibers have $E = 8.2$ GPa, $\sigma^* = 77$ MPa and a strain to failure of 1.4% (Ezekiel Mushi, Butchosa, Zhou, & Berglund, 2014). Compared with cellulose nanopaper ($E = 13$ GPa, $\sigma^* = 214$ MPa and strain to failure = 10%), these are still low values (Henriksson, Berglund, Isaksson, Lindström, & Nishino, 2008). We need improved understanding of the difference in characteristics of cellulose and chitin nanofibers. In particular, the low strain to failure of chitin membrane structures is difficult to understand.

For cellulose nanofibers, nanopaper strength correlates with cellulose molar mass for enzymatically extracted nanofibers (Henriksson et al., 2008) and to nanofiber length for TEMPO (2, 2, 6, 6-Tetramethylpiperidin-1-yl oxy) treated nanofibers (Fukuzumi, Saito, & Isogai, 2013). For chitin nanofiber extraction, enzymatic treatments are possible (Shimahara & Takiguchi, 1988), although the treatment time can be very long. This may be related to low accessibility of the proteins. Deacetylated (73% degree of acetylation) and depolymerized chitin nanowhiskers with small diameter (4–6 nm) and reduced length (110–400 nm) were obtained for 90 °C extraction temperature and 33% NaOH concentration (Fan et al., 2010). In another milder protocol for deproteinization at low NaOH-concentration (8%), (Ezekiel Mushi, Butchosa, Zhou, & Berglund, 2014; Ifuku et al., 2009; Ifuku, Nogi, et al., 2011a), long chitin-protein composite nanofibers were obtained with diameters from 10 to 30 nm. In both cases, the preparation times were shorter (4–48 h). The chitin microfibrils inside these larger nanofibers were not deacetylated, and the degree of acetylation was as high as 95%. However, it is worth to note that this relatively higher value was calculated by comparing the C and N content from elemental analysis data of chitin nanofibers that contain protein residues. It is challenging to completely remove the '*strongly bound*' protein fraction, without degradation of the chitin microfibrils. In biological organisms, protein and chitin are strongly associated with each other either covalently through aspartyl and histidyl linkages or non-covalently by β-sheet arrangements (Blackwell & Weih, 1980; Raabe et al., 2005).

An interesting approach to chitin nanofiber extraction is to operate at low temperature. Temperatures below 50 °C were suggested for insects in order to avoid depolymerization (Percot, Viton, & Domard, 2003). In the present study, low temperature deproteinization was therefore studied in order to remove the strongly 'bound' protein from the exoskeleton and preserve the microfibril structure i.e. degree of acetylation, molar mass, fiber width and fiber length. The present study is based on lobster exoskeletons, but it is possible that the success of the procedure depends on the specific organism used. Since chitin membrane structures are prepared by filtration from hydrocolloidal suspensions, it is important to avoid nanofiber agglomeration in the colloid, since this will lead to formation of agglomerated particles, which decrease mechanical strength properties and optical transparency of the membrane structure.

2. Materials and methods

2.1. Materials

Fresh frozen lobster (*Homarus americanus* from the Northwest Atlantic, produced in Canada) were purchased from the market in Stockholm (CoopExtra, Sweden) and used as the starting materials. The exoskeleton was about 14 wt.% of the whole lobster, measured after freeze drying. The whole lobster was cleaned to remove tissues and salts. The exoskeleton was freeze dried and ground to smaller than 35 mesh size in a Retsch grinder, Model ZM200 from Germany, to increase surface area for further chemical and mechanical treatments.

2.2. Disintegration of chitin nanofiber from lobster exoskeleton

A schematic diagram of the treatment steps is illustrated in Fig. 1. Extraction of minerals, pigments and proteins from the exoskeleton was done in the following order. Typically, 40 g lobster exoskeleton powder was first demineralized in 600 mL of 2 M HCl for 2 h. Subsequently, it was immersed in 300 mL of 96% ethanol and stirred overnight to remove the pigments. Finally, NaOH treatment was carried out to remove protein. Two different NaOH concentrations (8% and 20%) were used and the treatment duration was either 48 h or 2 weeks. The samples were designated as L8-48, L8-2W, L20-48 and L20-2W according the final deproteinization procedure. All treatments were carried out at room temperature (21 °C) and washing was performed with deionized water between each step until neutral pH was reached. After NaOH treatment, the exoskeleton powder was suspended in 1 L of 1–4% acetic acid and stirred overnight. The colloidal suspension (1 wt.%) was then blended at pH 3 using a powerful kitchen blender (VM0105E, USA) and passed 10 times through the microfluidizer (M-110EH, Microfluidics Ind., Newton, MA, USA), including first five passes through 400 and

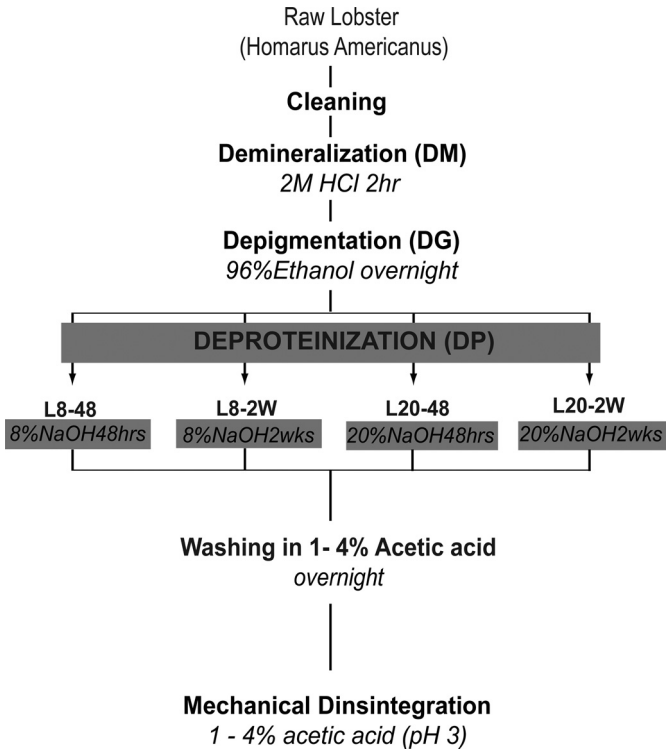

Fig. 1. Schematic diagram showing the extraction and disintegration steps for the preparation of chitin nanofibers from raw lobsters.

200 μm chambers at a pressure of 900 bar and five last passes through 200 and 100 μm chambers at a pressure of 1600 bar.

2.3. Characterization of chitin nanofibers

The following characterizations of chitin nanofiber were performed. The degree of deacetylation (DA) of the chitin nanofibers was measured by cross-polarization/magic angle spinning ^{13}C nuclear magnetic resonance (CP/MAS ^{13}C NMR) method as reported in our previous work (Butchosa et al., 2013). The DA value was determined by dividing the intensity of the resonance signal arising from the carbon of the methyl group by the intensity of the resonance signal corresponding to *C1* of the sugar ring. The residual protein content was determined based on a colorimetric method (Ninihydrin-hydridantin protein test) by Shimahara and Takiguchi (1988) as reported in our previous work (Ezekiel Mushi et al., 2014). Intrinsic viscosity [η] was measured in 8% LiCl/DMAc by using Ubbelohde capillary viscometer at room temperature (21 °C). The viscosity molar mass of chitin was calculated using Eq. (1) adopted from Terbojevich, Cosani, Bianchi, and Marsano (1996) based on Mark–Houwink relationship. Atomic force microscopy (AFM) of chitin nanofibers was performed on a mica substrate using Nanoscope IIIa (Veeco Instruments, Santa Barbara, USA) at ambient conditions (21 °C). Dilute suspension (0.005 wt.%) of the completely individualized nanofibers was dried on the mica substrates. AFM images were captured under tapping mode using RTESP silica cantilevers (Veeco) with a spring constant of 40 N m^{-1} and a tip radius of 8 nm oscillating at their fundamental resonance frequencies between 200 and 400 kHz. The heights of the chitin nanofibers, which are not subject to peak broadening artifacts, were used for estimation of width. A sample size of 300 nanofibers was used for all the calculations. Chitin membranes (see below for preparation procedure) were analyzed by X-ray diffraction (XRD) with a Philips X'Pert Pro Diffractometer (Model PW 3040/60) using CuKα radiation (λ = 1.5418 Å), which was generated at 45 kV and 35 mA and monochromatized using a 20 μm Ni filter. Diffractograms were recorded at room temperature in the reflection mode in the range from 5° to 40° (2θ angular range). The diffractograms were curve fitted to obtain crystal size and crystallinity index. The crystal size in (0 2 0) and (1 1 0) planes were measured from the widths at half-heights using Scherrer's equation (Fan, Saito, & Isogai, 2007), and crystallinity index calculated from the ratio of diffraction peak at 19.6° to the baseline at 16.0° (Fan et al., 2007). Scanning Transmission Electron Microscopy (STEM) of chitin nanofibers was performed using Field Emission Scanning Electron Microscope (FE-SEM) (S-4800 Hitachi, Japan) equipped with transmitted electron detector. Chitin nanofibers were deposited on a carbon coated copper grid and stained with uranyl acetate to elucidate the protein distribution. The STEM images were captured at 30 kV. Structural characteristics of chitin membranes (see below for preparation procedure) were also studied by using the FE-SEM (Hitachi S-4800, Japan). The membranes were dried and then sputtered with a thin layer of platinum/palladium using Agar HR sputter coater. FE-SEM images were captured from secondary electrons at 1.0 kV.

$$[\eta] = 2.1 \times 10^{-4} M^{0.88} \quad (1)$$

2.4. Preparation of nanostructured chitin membranes

A colloidal suspension of chitin nanofibers (about 0.07 wt.%) was mixed using an Ultra Turrax mixer (IKA, D125 Basic) for 10 min at 12,000 rpm to achieve a uniform dispersion. Thereafter, it was vacuum filtered using a filter funnel (Φ 7.2 cm) with a filter membrane (0.65 μm DVPP, Millipore, USA) to obtain a wet cake, which was then dried rapidly in a semi-automated paper making equipment (Rapid Köthen, Germany) according to the procedure reported by Sehaqui, Liu, Zhou, and Berglund (2010).

2.5. Characterization of nanostructured chitin membranes

Tensile test was performed in uniaxial tension using an Instron Universal Tensile Testing Machine equipped with a load cell of 500 N (Model 5944, UK). The specimens were conditioned overnight at 50% relative humidity and 23 °C prior to testing. The specimen size was 60 mm in length and 5 mm in width. The thickness was measured each time from three random points and averaged thickness was in range of 50–60 μm. Tensile test was performed at a strain rate of 4 mm/min and a gauge length of 40 mm. Mechanical properties measured include tensile modulus, tensile strength, strain-to-failure, and work to fracture, which is proportional to the area under the stress–strain curve. Porosity determination was carried out based on density method reported previously by using Mercury Intrusion Porosimetry (Micromeritics, USA) (Ezekiel Mushi et al., 2014). Regular light transmittance was measured on colloidal suspension and chitin membranes over the wavelength range from 200 to 800 nm using UV-Vis Spectrophotometer (UV-2550, Shimadzu Corporation, Japan). The suspension of chitin nanofibers with 6% protein content from L8-2W (not shown) showed low transmittance compared to L8-48, possibly due to contamination. The membrane was dried in air at room temperature (21 °C) before transmittance test.

3. Results and discussion

3.1. Disintegration of chitin nanofibers from lobster exoskeleton

Strong acid hydrolysis results in short chitin whiskers, and very mild treatment result in thick chitin nanofiber bundles with high residual protein content. The disintegration protocol developed in this work aims to address this enigma and preserve the chemical and structural properties of chitin nanofibers in the biological organism. The procedure is presented in Fig. 1. Based on previous methods for demineralization: very mild (Percot et al., 2003) or more severe (Ifuku et al., 2010), a compromise was selected. The inorganic components were removed during 2 h treatment using 2 M HCl aqueous solution, with a ratio of 15 mL HCl solution per g of lobster exoskeleton powder. This treatment is fairly mild in order to minimize chitin hydrolysis. For the removal of pigments, ethanol was used at a ratio of 15 mL ethanol per g of the lobster exoskeleton powder. The best order of treatments was found to be demineralization, depigmentation and deproteinization. The NaOH treatment for the removal of proteins was varied as shown in Fig. 1. The yield of this step was between 75% and 84% depending on NaOH concentration and treatment time. The protein removed during the first 48 h was termed *weakly bound protein*. Washing in acetic acid overnight removed remaining discoloration. Acetic acid may penetrate and swell chitin-protein fibril bundles and facilitate mechanical disintegration. This is based on Park, Marsh, and Rhim (2002). White color of the exoskeleton correlated with translucent and stable hydrocolloids after homogenization, see Fig. 1.

3.2. Chemical properties of chitin nanofibers

Table 1 shows the values of degree of acetylation, residual protein content, and intrinsic viscosity or molar mass for the chitin nanofibers after isolation. Protein removal usually leads to chitin deacetylation and hydrolysis. The present challenge is to prepare very small diameter chitin nanofibers of low protein content, with preserved molar mass and degree of acetylation. NaOH treatment at room temperature has been used. The resulting nanofibers showed the same degree of acetylation, 86%, as determined by solid state

Table 1
Chemical characteristics of chitin nanofibers including degree of acetylation, protein content, intrinsic viscosity and molar mass.

Sample description	Degree of acetylation (%)	Protein content (%)	Intrinsic viscosity (dl/g)	Viscosity molar mass, M_v (Da)
L8-48	86	12.4 (3.5)	33.3 (6.7)	811,600
L8-2W	86	6.0 (4.3)	26.5 (5.6)	626,100
L20-48	87	7.1 (6.4)	29.7 (5.8)	753,300
L20-2W	86	4.7 (3.5)	23.4 (7.5)	543,500

Note: The number in brackets is standard deviation.

^{13}C NMR, regardless of NaOH concentration or amount of protein removed. This is similar to results for α-chitin from crab by solid state ^{13}C NMR, 89.8% (Van de Velde & Kiekens, 2004). The value for degree of acetylation depends on species and measurement technique. Degree of acetylation of chitin from the fungus *Aspergillus niger* is 80% as determined from analysis of acetic acids hydrolysate by high-performance liquid chromatography (Wu, Zivanovic, Draughon, Conway, & Sams, 2005). Ifuku et al. (2010) and Fan et al. (2008) reported degree of acetylation of around 96 and 93%, respectively, for crab shell chitin as determined by elemental analysis. Certainly, the degree of acetylation is largely preserved and most of the strongly '*bound*' protein is removed based on this protocol. In Table 1, the intrinsic viscosity decreases with decreased protein content. This is because the protein increases the viscosity, rather than an effect from reduced chitin molar mass. At very small values for residual protein (i.e. 4.7%), the value of intrinsic viscosity corresponds to ca. 543.5 kDa molar mass of chitin. Our results are in the range of viscosity molar mass of chitin from honeybee corpses, measured in DMAc/5% LiCl, after treatment in 1 M NaOH at 80 °C for different times between 1.5 and 2.5 days (Draczynski, 2008). The values reported were between 420 and 740 kDa. The molar mass of chitin reported in other literature ranged from 600 kDa (Mima, Miya, Iwamoto, & Yoshikawa, 1983) to 1050 kDa from crab shell by light scattering (Hackman & Goldberg, 1974). The present estimate of chitin molar mass indicates that there is no strong reduction in chitin molar mass due to hydrolysis effects. Some molar mass reduction is expected, simply from nanofiber fractures during mechanical homogenization.

3.3. Structural properties of chitin nanofibers

The histograms in Fig. 2 show the distribution of chitin nanofiber length and width for different treatment conditions. Lower protein content correlates with smaller diameter and shorter nanofiber lengths (compare L8-48 with the lower protein content L20-2W nanofibers). In particular, the very large diameter nanofibers are absent in L20-2W. The nanofibers are unique in terms of the small diameter and low protein content. At high NaOH concentration (20%), the length ranged from 200 to 2000 nm. The heterogenity of data was estimated as weight average to number average ratios (Hull & Clyne, 1981). The width heterogenity is 1.1, which means the fibril widths were quite uniform. This indicates that the diameter of the present nanofibers is controlled by biosynthesis, and may indeed correspond to chitin microfibrils.

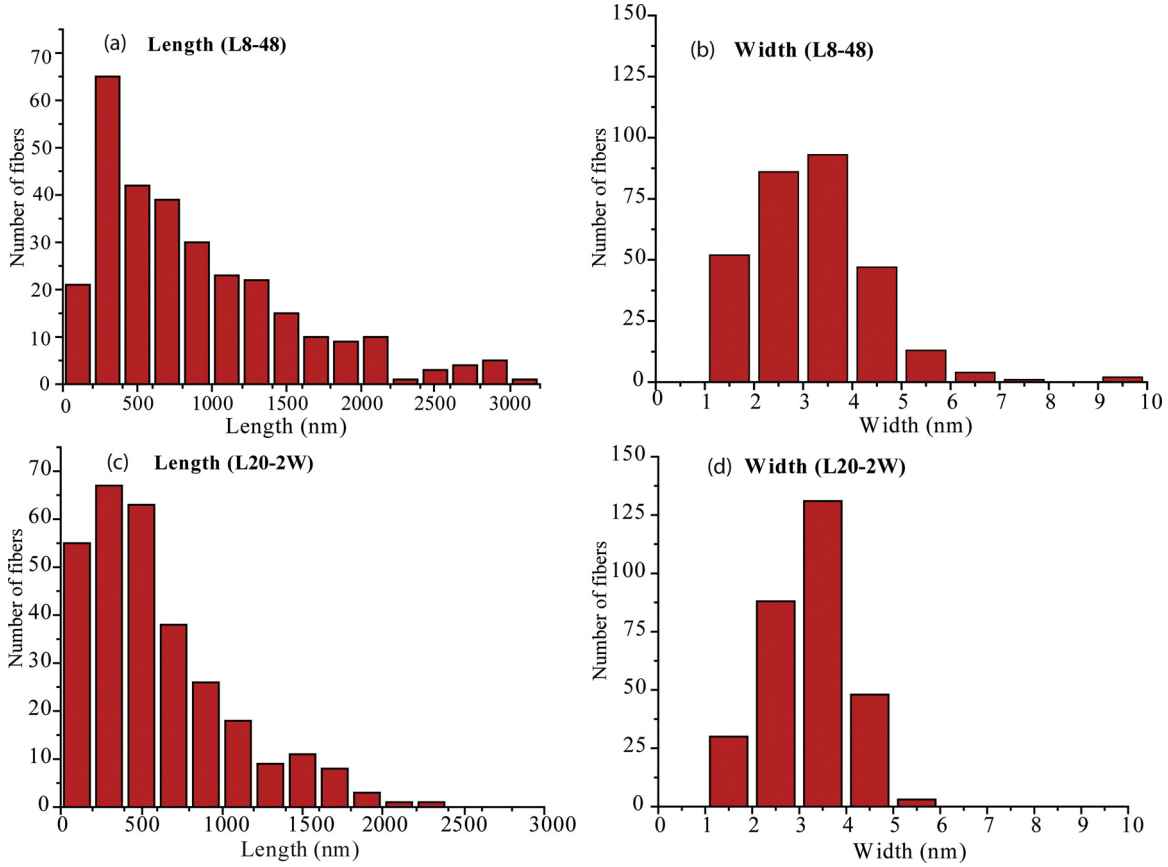

Fig. 2. Histograms showing length (a, c) and width (b, d) distribution of 300 chitin nanofibers each isolated from lobster exoskeleton: (a, b) L8-48 (8% NaOH deproteinization for 48 h) and (c, d) L20-2W (20% deproteinization for 2 weeks).

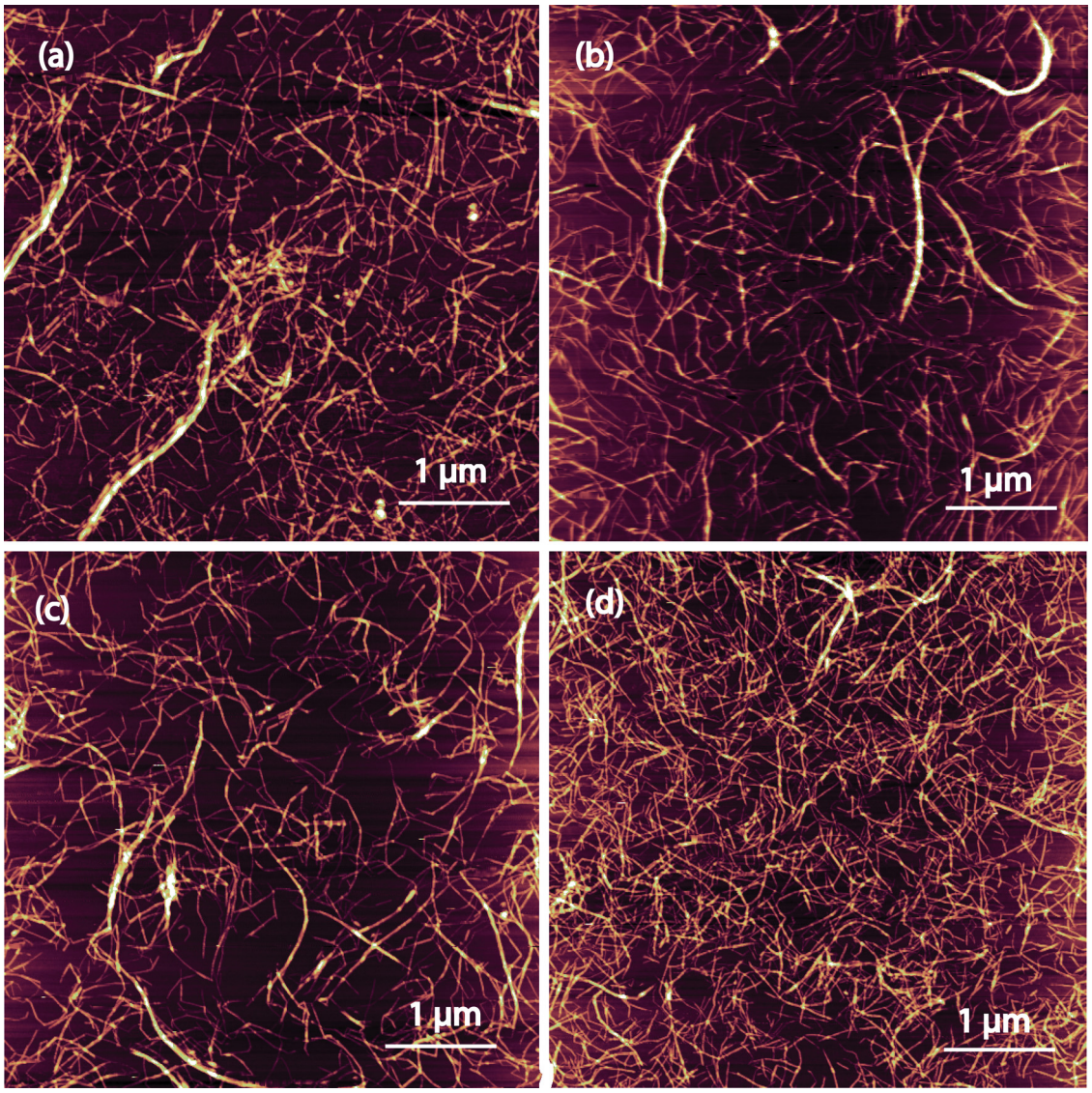

Fig. 3. AFM images of chitin nanofiber structures: (a) L8-48, (b) L8-2W, (c) L20-48, and (d) L20-2W. L8-48 was treated in 8% NaOH for 48 h and L8-2W for 2 weeks. L20-48 corresponds to 20% NaOH for 48 h and L20-2W for 2 weeks.

The chitin nanofiber structure is also presented in AFM images, see Fig. 3. For shorter treatment times or low NaOH concentration, larger diameter protein-containing chitin nanofiber bundles are apparent, see AFM height images in Fig. 3(a–c). The L20-2W sample treated for the longest time also shows the most homogeneous width distribution, see Fig. 2(d) and Fig. 3(d). Table 2 presents a summary of length and width of chitin nanofiber from lobster, based on AFM images (not presented) and XRD data (not shown). Chitin crystal structure from XRD was deduced at (1 1 0) and (0 2 0) plane. The crystal structure dimension along (1 1 0) plane is different from that along plane (0 2 0). Similar results along crystal planes of chitin were reported for deacetylated chitin nanowhiskers from crabs (Fan et al., 2007, 2012). It was 6.7 nm along plane (1 1 0) and 9.6 nm along (0 2 0). Chitin fibril width from AFM i.e. 3 nm are slightly lower compared to the size obtained from XRD i.e. between 4.0 and 5.6 nm. The STEM image in Fig. 4 presents individual fibrils in more detail. The lighter entities are individualized chitin nanofibers. The length of individual fibrils in STEM and AFM images

Table 2
Length and width of chitin nanofibers by AFM and XRD.

Sample description	Protein content (%)	AFM						XRD		C.I. (%)
		Length (nm)			Width (nm)			Crystal size (nm)		
		l_n	l_w	l_w/l_n	d_n	d_w	d_w/d_n	$D_{(110)}$	$D_{(200)}$	
L8-48	12.4 (3.5)	966	1411	1.46	3.5	3.9	1.11	4.0	5.1	89
L8-2W	6.0 (4.3)	1167	1526	1.31	3.1	3.4	1.09	4.1	5.6	89
L20-48	7.1 (6.4)	906	1240	1.37	3.4	3.8	1.12	4.6	5.4	90
L20-2W	4.7 (3.5)	697	1025	1.47	3.4	3.6	1.06	4.1	4.8	89

Note: l_n – number average length. l_w – weight average length. d_n – number average width. d_w – weight average width. l_w/l_n and d_w/d_n stand for polydispersity or heterogeneity. $d_{(110)}$ – crystal size along plane (1 1 0), $d_{(200)}$ – crystal size along plane (2 0 0), C.I. – crystallinity index. The number in brackets is standard deviation.

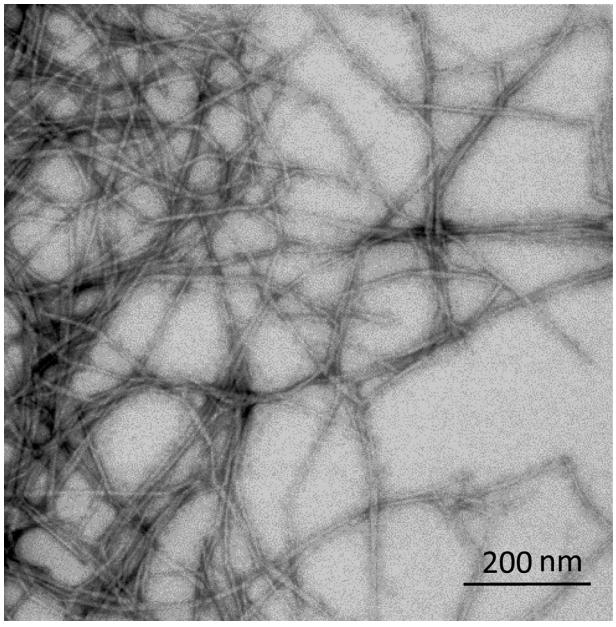

Fig. 4. STEM image of low protein chitin nanofiber structures: sample L20-2W (20% NaOH for 2 weeks).

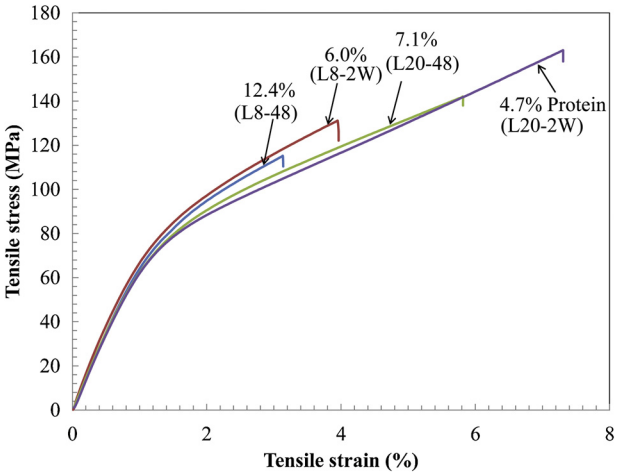

Fig. 5. Tensile stress–strain curves of porous chitin nanofiber membranes. Treatment conditions are indicated in parenthesis, see Table 1.

are almost identical. The nanofiber width from STEM in Fig. 4 is similar to the fibril width from AFM. The width of the crystal structure, especially along plane (1 1 0), closely corresponds to the nanofiber width from AFM and STEM.

Structural distribution with respect to length and width of nanofibers can be related to the amount of residual protein. The decrease in protein content was correlated with a larger fraction of small diameter fibril bundles and much shorter fibrils. At 20% NaOH, the protein concentration was ca. 4.7% and the degree of acetylation was the same as for samples treated under milder NaOH concentration. Small diameter individualized chitin nanofibers (corresponding to microfibrils) are then dominating the sample. The geometrical similarity with crystal structure from XRD or the stained fibrils characterized by STEM is striking. This strongly suggests that the original chitin microfibril structure was isolated and preserved in the present disintegration protocol. According to literature, the diameter of the chitin crystal structure is between 3 and 6 nm and the length from 300 to 500 nm (Blackwell & Weih, 1980; Raabe et al., 2005). In TEMPO α-chitin nanocrystals, a diameter of ca. 8–10 nm and length up to 340 nm was reported (Fan et al., 2007). Fibril length and degree of deacetylation are higher in the current chitin fibrils than reports for deacetylated nanowhiskers of the same diameter i.e. 3–4 nm from crab shell (Fan et al., 2007, 2010, 2012). Prior to the present study, it is only β-chitin nanofibers from tubeworms or squids, and isolated through mild NaOH treatment, which have shown similar small diameters, large fiber lengths and high degrees of acetylation (Fan et al., 2010, 2012). Diameter of β-chitin nanofibers from squid ranged from 3 to 4 nm with lengths in the micron-scale (Fan et al., 2008, 2012).

3.4. Chitin membrane properties and structure

Chitin membranes were prepared from the wet cake of chitin nanofiber hydrocolloids based on Sehaqui et al. (2010). Mechanical, structural and optical properties are presented in Figs. 5–7. Fig. 5 shows the stress–strain behavior of nanostructured chitin membranes. Tensile modulus, strength, strain to failure and work to fracture are presented in Table 3. The term "strain hardening modulus" is used to describe the slope of the stress–strain curve in the post-yield region where strain-hardening behavior is apparent, see Fig. 5. The slope is determined from a best fit to stress–strain data so that the unit of strain hardening modulus becomes GPa. Compared with previous mechanical property data for chitin membranes based on chitin nanofibers with higher protein content and larger diameter (Ezekiel Mushi et al., 2014; Ifuku & Saimoto, 2012), the present tensile properties are superior. In particular, strain to failure and work to fracture is much improved. The stress–strain behavior of the present membranes is characterized by an initial linear region, then a plastic yielding "knee", followed by strain-hardening at constant stress–strain slope. Plastic deformation is due to interfibril slippage rather than plastic deformation in the nanofibers themselves. Compared with the previous study (Ezekiel Mushi et al., 2014), the strain-to-failure increased. For the present type of stress–strain behavior, this leads to increased ultimate tensile strength and work to fracture (area under stress–strain curve).

The present chitin membranes show higher strength and in particular strain-to-failure (higher ductility) than those in previous studies. Data for the present materials (nanofiber dimensions, optical transmittance) indicate that the more brittle materials with lower strain-to-failure have a structure with a substantial amount of nanofiber agglomerates. In Fig. 6, FE-SEM images of membrane surface topography are presented. Fig. 6(a) presents larger chitin nanofiber bundles, whereas the structure in Fig. 6(b) has a larger fraction of individualized, small diameter chitin nanofibers. The reason for the presence of some larger nanofiber bundles in Fig. 6(a) is that the NaOH treatment conditions are "too mild" with lower concentration (8% rather than 20%) and shorter treatment time (48 h rather than 2 weeks). Larger nanofiber bundles and agglomerates are likely to act as sites of stress concentration. Microscale cracks may thus form at low strain, and cause premature failure and low strength.

Optical transmittance data for the chitin nanofiber colloidal suspensions also indicate that nanofibers with shorter treatment times and higher protein content contain more agglomerates, see Fig. 7(a). The nanofiber suspension with the lowest protein content shows the highest optical transmittance. See Fig. 7(b) for an image of the low protein chitin nanofiber hydrocolloid. The transmittance depends on the diameter of suspended nanofibers (Fukuzumi, Saito, Iwata, Kumamoto, & Isogai, 2008). It is likely that the nanofibers with higher protein content have a fraction of large diameter nanofibers, which may also promote formation of agglomerates already in the colloidal state. Optical transmittance data for membranes are also in support of the agglomeration hypothesis, see Fig. 7(c). Fig. 7(d) presents a photographical image of a low protein chitin membrane. It is very transparent even by visual inspection.

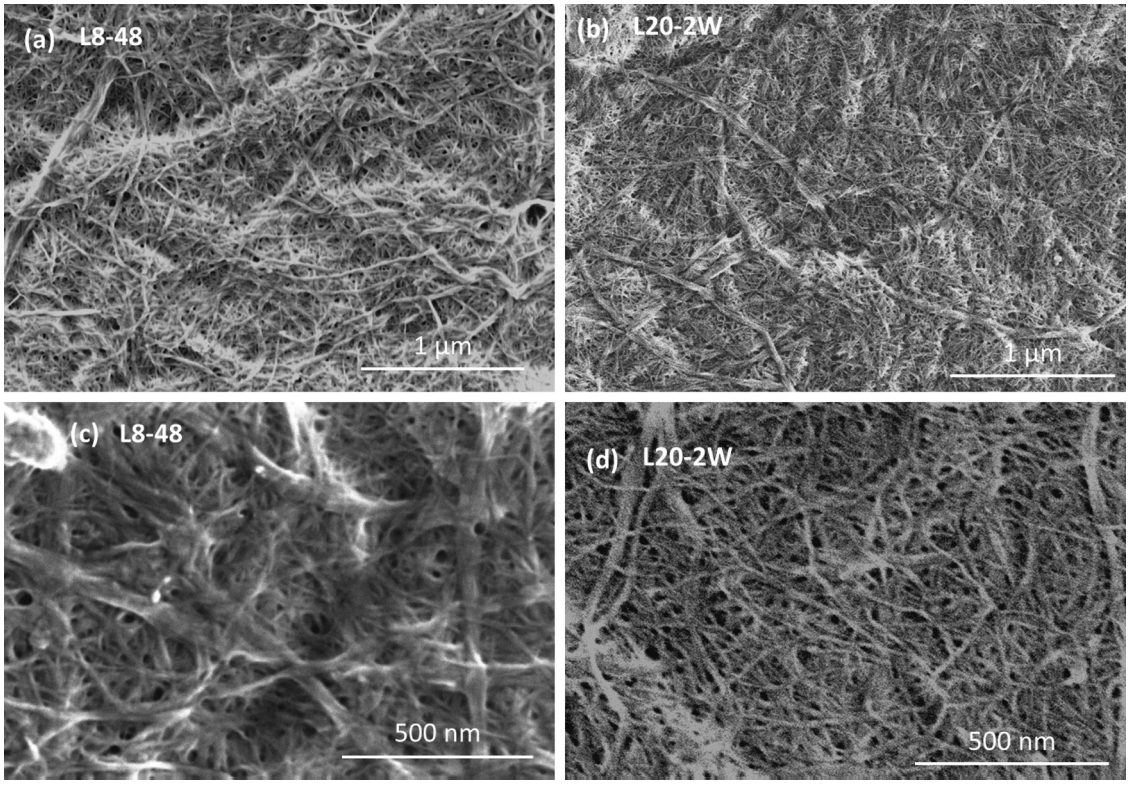

Fig. 6. SEM images of chitin membranes from chitin nanofibers at 1 μm and 500 nm scale bars: (a, c) L8-48 (8% NaOH, 48 h), and (b, d) L20-2W (20% NaOH, 2 weeks).

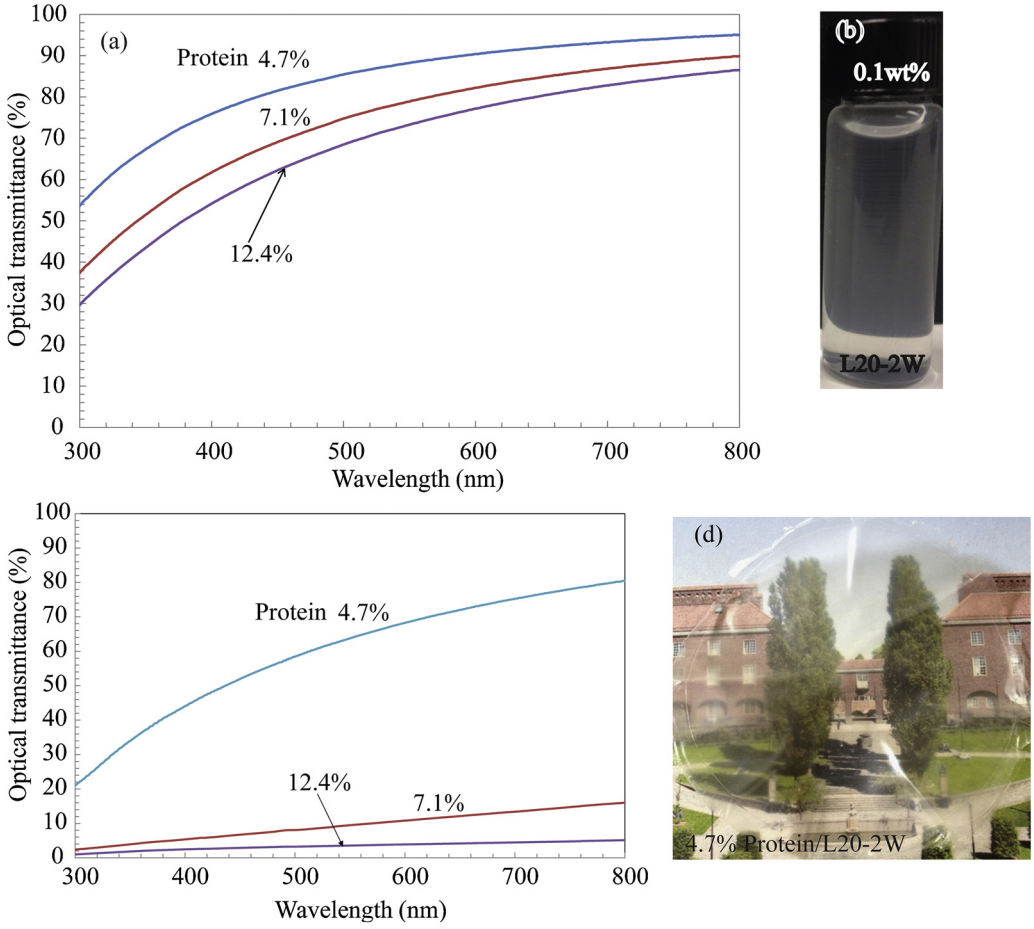

Fig. 7. Regular optical transmittance of chitin nanofibers: (a) transmittance curves from 0.1 wt.% suspension, (b) chitin nanofiber hydrocolloids at 0.1 wt.%, (c) transmittance curves from chitin membranes, and (d) low protein chitin membrane (L20-2W).

Table 3
Tensile properties of chitin membranes including data for treatment conditions, protein content, density and porosity.

Parameters	Chitin membrane properties			
NaOH treatment condition	8%–48 h	8%–2 weeks	20%–48 h	20%–2 weeks
Protein content (%)	12.4 (3.5)	6.0 (4.3)	7.1 (6.4)	4.7 (3.5)
Density (g/cm^3)	1.18	1.09	1.10	1.21
Porosity (%)	17	24	23	16
Tensile modulus (GPa)	7.8 (0.3)	7.9 (0.5)	8.3 (0.8)	7.3 (0.4)
Tensile strength (MPa)	107 (8.9)	140 (7.6)	141 (7.7)	153 (10.6)
Yield strength (MPa)	72 (5.0)	74 (5.5)	73 (1.3)	70 (1.6)
Tensile strain to failure (%)	3.9 (0.9)	5.7 (1.1)	5.7 (0.4)	8.0 (1.0)
Strain-hardening modulus (GPa)	1.1 (0.6)	1.9 (0.7)	1.4 (0.2)	1.4 (0.1)
Work to fracture (MJ/m^3)	1.9 (0.6)	5.8 (0.5)	6.1 (0.8)	8.3 (0.2)

Note: The number in brackets is standard deviation.

Table 4
Comparison of tensile properties of chitin membranes.

Description (authors)	Degree of acetylation (%)	Young's modulus (GPa)	Tensile strength (MPa)	Tensile strain to failure (%)
Our current results	86 (NMR)	7.3	153	8.0
Ezekiel Mushi et al. (2014)	95 (FT-IR)	8.2	77	1.4
Ifuku et al. (2013)	Deacetylated*	8.8	157	–*
Ifuku and Saimoto (2012)	96** (Elemental)	3.0	44	–*
Fan et al. (2010)	74 (Elemental)	5.0	140	10

Note: * Value was not reported; ** Degree of acetylation (Elemental analysis) by Ifuku et al. (2010). The text in brackets represents a measurement technique.

The high protein content structures show very poor transmittance, indicating the presence of agglomerated nanofibers. The fraction of large nanofiber bundles is small and difficult to quantify, but may have a very strong effect on properties. Perhaps larger agglomerates in the form of "flocs" (Farnood, Loewen, & Dodson, 1994) are formed, for instance, during filtration when the nanofiber concentration is locally increased in the vicinity of the filter membrane surface.

In previous studies of α-chitin-based films (Fan et al., 2012), the optical transparency is higher than in the present study. Their nanofibers were highly derivatized with a high degree of deacetylation (i.e. 27%). The chitin nanofiber surfaces then have chitosan characteristics, including high charge, which enhances nanofiber dispersion in colloids. In contrast, the goal of the present work was to preserve as much of the original chitin microfibril structure as possible.

Data in Table 4 compares tensile properties of chitin membranes with other materials. In a previous study on structures from larger diameter chitin-protein composite nanofibers, we reported on a content of 7% of residual protein in the composite nanofibers (Ezekiel Mushi et al., 2014). The mechanical properties in tension were much inferior to the present study. The tensile strength was 77 MPa, and the strain to failure only 1.4%. Tensile strengths of films based on larger diameter chitin nanofibers were also lower than present data (Ifuku & Saimoto, 2012). The intrinsic properties of the present chitin nanofibers (L20-2W) should be better than in our previous study, due to higher purity, smaller diameter and better preserved chitin molar mass and fibril length. Moreover, the shape of the present stress–strain curves also demonstrates that high strain to failure is essential in order to reach high ultimate strength. The finer structure of present nanofibers and membranes is important for this achievement. The best mechanical properties in previous studies were from highly deacetylated chitin nanowhiskers/nanofibers (Fan et al., 2012; Ifuku et al., 2013), where the strongly bound protein was completely removed. Higher protein content is associated with lower degree of nanofiber dispersion, larger agglomerates and lower strain to failure. See Table 3 for the relationship of tensile strain to failure with residual protein content. One may speculate that the presence of protein provides strong interaction between nanofibers so that plasticity mechanisms such as interfibril slippage become more difficult. The value of modulus remained more or less unchanged whether chitin nanofiber were completely individualized or not. Modulus is measured at small strain, and is controlled by nanofiber orientation distribution, porosity and fiber–fiber bonding. The lack of modulus variation is because none of these parameters are likely to be strongly influenced by protein content. In the present work, finer structures of chitin nanofibers were achieved compared with previous studies and at a much higher degree of acetylation, and lower protein content. This correlated with improved mechanical properties in uniaxial tensile tests.

4. Conclusions

Previous studies report on preparation of chitin-protein composite nanofibers or deacetylated chitin nanofibers (chitosan surface with preserved native chitin core). In contrast, the present study reports on a mild extraction procedure by which low protein individualized chitin nanofibers are isolated from Crustaceans. The chemical and physical structures of the isolated nanofibers appear similar to the chitin microfibrils in the biological organism. Deacetylation is negligible and nanofiber lengths are substantial, indicating only limited hydrolysis effects. The nanofibers have very small diameter (weight average width = 3.6–3.9 nm), are very long (weight average length = 1.0–1.5 μm) and show a swirled structure in the chitin nanofiber networks. This facilitates formation of mechanical entanglements in the network structure. The mechanical tensile properties of the present α-chitin membranes are the highest reported for materials from non-derivatized chitin nanofibers. In particular, the present membranes are very ductile, with a strain to failure as high as 8%. The network nanostructure micrographs and optical transmittance data provide the major explanation for the correlation between lowered protein content and improved mechanical properties. High chitin content correlates with fewer large nanofiber agglomerates, and better optical transmittance for both nanofiber suspensions and membranes. Also, high chitin content membrane structures have the highest strength and toughness (area under stress–strain curve) due to a lower content of agglomerates. It is becoming clear that low protein chitin nanofibers, in very similar state as in the biological organism, have geometrical and mechanical properties of great

interest. Furthermore, the unique surface chemistry of pure chitin provides opportunity for tailoring of functionalities in nanomaterials such as polymer matrix nanocomposites, aerogels, hydrogels and organic–inorganic hybrid materials.

Acknowledgements

The authors of this work gratefully acknowledge financial support from the Carbomat Project funded by Formas. Assoc. Prof. Tsuguyuki Saito from Department of Biomaterial Sciences at the University of Tokyo in Japan contributed to interpretation of the XRD data.

References

Blackwell, J., & Weih, M. (1980). Structure of chitin-protein complexes: Ovipositor of the ichneumon fly Megarhyssa. *Journal of Molecular Biology*, *137*(1), 49–60.

Butchosa, N., Brown, C., Larsson, P. T., Berglund, L. A., Bulone, V., & Zhou, Q. (2013). Nanocomposites of bacterial cellulose nanofibers and chitin nanocrystals: Fabrication, characterization and bactericidal activity. *Green Chemistry*, *15*(12), 3404–3413.

Draczynski, Z. (2008). Honeybee corpses as an available source of chitin. *Journal of Applied Polymer Science*, *109*(3), 1974–1981.

Ezekiel Mushi, N., Butchosa, N., Zhou, Q., & Berglund, L. A. (2014). Nanopaper membranes from chitin–protein composite nanofibers—Structure and mechanical properties. *Journal of Applied Polymer Science*, *131*(7) http://dx.doi.org/10.1002/APP.40121

Fan, Y., Fukuzumi, H., Saito, T., & Isogai, A. (2012). Comparative characterization of aqueous dispersions and cast films of different chitin nanowhiskers/nanofibers. *International Journal of Biological Macromolecules*, *50*(1), 69–76.

Fan, Y., Saito, T., & Isogai, A. (2007). Chitin nanocrystals prepared by TEMPO-mediated oxidation of α-chitin. *Biomacromolecules*, *9*(1), 192–198.

Fan, Y., Saito, T., & Isogai, A. (2008). Preparation of chitin nanofibers from squid pen β-chitin by simple mechanical treatment under acid conditions. *Biomacromolecules*, *9*(7), 1919–1923.

Fan, Y. M., Saito, T., & Isogai, A. (2010). Individual chitin nano-whiskers prepared from partially deacetylated α-chitin by fibril surface cationization. *Carbohydrate Polymers*, *79*(4), 1046–1051.

Farnood, R. R., Loewen, S. R., & Dodson, C. (1994). Estimation of intra-floc forces. *Appita*, *47*(5), 391–396.

Fukuzumi, H., Saito, T., & Isogai, A. (2013). Influence of TEMPO-oxidized cellulose nanofibril length on film properties. *Carbohydrate Polymers*, *93*(1), 172–177.

Fukuzumi, H., Saito, T., Iwata, T., Kumamoto, Y., & Isogai, A. (2008). Transparent and high gas barrier films of cellulose nanofibers prepared by TEMPO-mediated oxidation. *Biomacromolecules*, *10*(1), 162–165.

Giraud-Guille, M.-M. (1984). Fine structure of the chitin-protein system in the crab cuticle. *Tissue and Cell*, *16*(1), 75–92.

Hackman, R. H., & Goldberg, M. (1974). Light-scattering and infrared spectrophotometric studies of chitin and chitin derivatives. *Carbohydrate Research*, *38*, 35–45.

Henriksson, M., Berglund, L. A., Isaksson, P., Lindström, T., & Nishino, T. (2008). Cellulose nanopaper structures of high toughness. *Biomacromolecules*, *9*(6), 1579–1585.

Hull, D., & Clyne, T. (1981). *An introduction to composite materials* (1st ed.). New York, USA: Cambridge University Press.

Ifuku, S., Ikuta, A., Egusa, M., Kaminaka, H., Izawa, H., Morimoto, M., et al. (2013). Preparation of high-strength transparent chitosan film reinforced with surface-deacetylated chitin nanofibers. *Carbohydrate Polymers*, *98*(1), 1198–1202.

Ifuku, S., Nogi, M., Abe, K., Yoshioka, M., Morimoto, M., Saimoto, H., et al. (2009). Preparation of chitin nanofibers with a uniform width as α-chitin from crab shells. *Biomacromolecules*, *10*(6), 1584–1588.

Ifuku, S., Nogi, M., Abe, K., Yoshioka, M., Morimoto, M., Saimoto, H., et al. (2011). Simple preparation method of chitin nanofibers with a uniform width of 10–20 nm from prawn shell under neutral conditions. *Carbohydrate Polymers*, *84*(2), 762–764.

Ifuku, S., Nogi, M., Yoshioka, M., Morimoto, M., Yano, H., & Saimoto, H. (2010). Fibrillation of dried chitin into 10–20 nm nanofibers by a simple grinding method under acidic conditions. *Carbohydrate Polymers*, *81*(1), 134–139.

Ifuku, S., Nomura, R., Morimoto, M., & Saimoto, H. (2011). Preparation of chitin nanofibers from mushrooms. *Materials*, *4*(8), 1417–1425.

Ifuku, S., & Saimoto, H. (2012). Chitin nanofibers: Preparations, modifications, and applications. *Nanoscale*, *4*(11), 3308–3318.

Kjartansson, G. T., Zivanovic, S., Kristbergsson, K., & Weiss, J. (2006). Sonication-assisted extraction of chitin from shells of fresh water prawns (*Macrobrachium rosenbergii*). *Journal of Agricultural and Food Chemistry*, *54*(9), 3317–3323.

Mima, S., Miya, M., Iwamoto, R., & Yoshikawa, S. (1983). Highly deacetylated chitosan and its properties. *Journal of Applied Polymer Science*, *28*(6), 1909–1917.

Neville, A. (1967). Chitin orientation in cuticle and its control. *Advances in Insect Physiology*, *4*, 213–286.

Ogawa, Y., Kimura, S., & Wada, M. (2011). Electron diffraction and high-resolution imaging on highly-crystalline β-chitin microfibril. *Journal of Structural Biology*, *176*(1), 83–90.

Park, S., Marsh, K., & Rhim, J. (2002). Characteristics of different molecular weight chitosan films affected by the type of organic solvents. *Journal of Food Science*, *67*(1), 194–197.

Percot, A., Viton, C., & Domard, A. (2003). Optimization of chitin extraction from shrimp shells. *Biomacromolecules*, *4*(1), 12–18.

Raabe, D., Sachs, C., & Romano, P. (2005). The crustacean exoskeleton as an example of a structurally and mechanically graded biological nanocomposite material. *Acta Materialia*, *53*(15), 4281–4292.

Rudall, K. (1963). The chitin/protein complexes of insect cuticles. *Advanced Insect Physiology*, *1*, 257–313.

Sehaqui, H., Liu, A., Zhou, Q., & Berglund, L. A. (2010). Fast preparation procedure for large, flat cellulose and cellulose/inorganic nanopaper structures. *Biomacromolecules*, *11*(9), 2195–2198.

Shimahara, K., & Takiguchi, Y. (1988). Preparation of crustacean chitin. *Methods in Enzymology*, *161*, 417–423.

Terbojevich, M., Cosani, A., Bianchi, E., & Marsano, E. (1996). Solution behavior of chitin in dimethylacetamide/LiCl. In A. Domard, C. Jeuniaux, R. A. A. Muzzarelli, & G. Roberts (Eds.), *Advances in chitin science* (Vol. 1) (pp. 333–339). Brest, France: Jacques André Pub.

Van de Velde, K., & Kiekens, P. (2004). Structure analysis and degree of substitution of chitin, chitosan and dibutyrylchitin by FT-IR spectroscopy and solid state ^{13}C NMR. *Carbohydrate Polymers*, *58*(4), 409–416.

Wu, T., Zivanovic, S., Draughon, F. A., Conway, W. S., & Sams, C. E. (2005). Physicochemical properties and bioactivity of fungal chitin and chitosan. *Journal of Agricultural and Food Chemistry*, *53*(10), 3888–3894.